Infrared Spectroscopy of the OH Stretching Vibrations of Jet-Cooled Salicylic Acid and Its Dimer in S_0 and S_1

Toru Yahagi, Asuka Fujii,* Takayuki Ebata, and Naohiko Mikami*

Department of Chemistry, Graduate School of Science, Tohoku University, Sendai 980-8578, Japan

Received: July 10, 2001; In Final Form: September 4, 2001

Infrared spectra of the OH stretching vibrations of the jet-cooled salicylic acid (SA) monomer and dimer were measured for both their electronic ground (S_0) and first excited (S_1) states. For the SA monomer, conformations of two rotational isomers (rotamers) which have been identified by the electronic transitions were determined on the basis of the infrared spectra with the help of theoretical calculations. The intramolecular hydrogen-bonded OH stretching vibrations of the monomer showed a drastic change upon the electronic excitation, and it was consistent with the distortion of the H-chelate ring in the S_1 state predicted by theoretical calculations of Sobolewski and Domcke (*Chem. Phys.* **1998**, *232*, 257). Structures of the dimer in the S_0 and S_1 states were also determined by the observation of the OH stretching vibrations. No evidence was found for intermolecular double proton-transfer both in the S_0 and S_1 states of the dimer.

I. Introduction

Salicylic acid (SA) is known to form an intramolecular hydrogen bond between neighboring hydroxyl and carboxyl groups. With respect to the internal rotation of the carboxyl group, two conformational isomers (rotamers) are expected, as schematically shown in Figure 1. In rotamer I, the phenolic OH acts as a proton donor to the carbonyl group, while the carboxylic OH is a proton acceptor in rotamer II. Because the carbonyl group is more basic than the carboxylic OH, the intramolecular hydrogen bond is expected to be stronger in rotamer I than in rotamer II. In condensed phases, however, since the SA monomer exists under an equilibrium condition with the stable cyclic dimer, substantial spectral overlaps with that of the dimer prevent us from a detailed study of the structure of the monomer.[1−9]

Bisht et al. applied supersonic jet spectroscopy to SA for the first time, and succeeded in observing the S_1-S_0 transitions of the SA monomer and the dimer, separately.[10] The SA monomer shows two band systems around 335 and 310 nm; the former system was assigned to the S_1-S_0 (π, π^*) transition of rotamer I. The latter was attributed to the S_1-S_0 (n, π^*) transition of rotamer II. These assignments were based on the similarity to the spectra of methyl salicylate (MS).[11−12] In addition, a dual fluorescence was observed for the excitation of the 335 nm system, and it was attributed to the excited-state intramolecular proton transfer (ESIPT) from the phenolic OH to the carbonyl group, as discussed later.

For the stable structure of the SA dimer, controversial ideas have long been discussed.[2,6−10,13,14] Dimerization of two monomers of rotamer I or of rotamer II leads to isomers A or B, respectively, as shown schematically in Figure 1. Though rotamer I is expected to be more abundant than rotamer II, the double proton transfer after the dimerization would enable rotamer I to form isomer B. While IR and NMR studies in condensed phases supported that isomer A is dominant, an emission study of crystalline SA suggested that the two isomers exist under an equilibrium.[6,8] The SA dimer in a supersonic expansion was also studied by Bisht et al.[10] In the electronic spectrum, they found many bands near the 335 nm system of rotamer I, and assigned them to the S_1-S_0 transitions of the SA dimer on the basis of the nozzle temperature (sample concentration) dependence of the band intensity. Later, Lahmani and Zehnacker-Rentien also observed fluorescence excitation

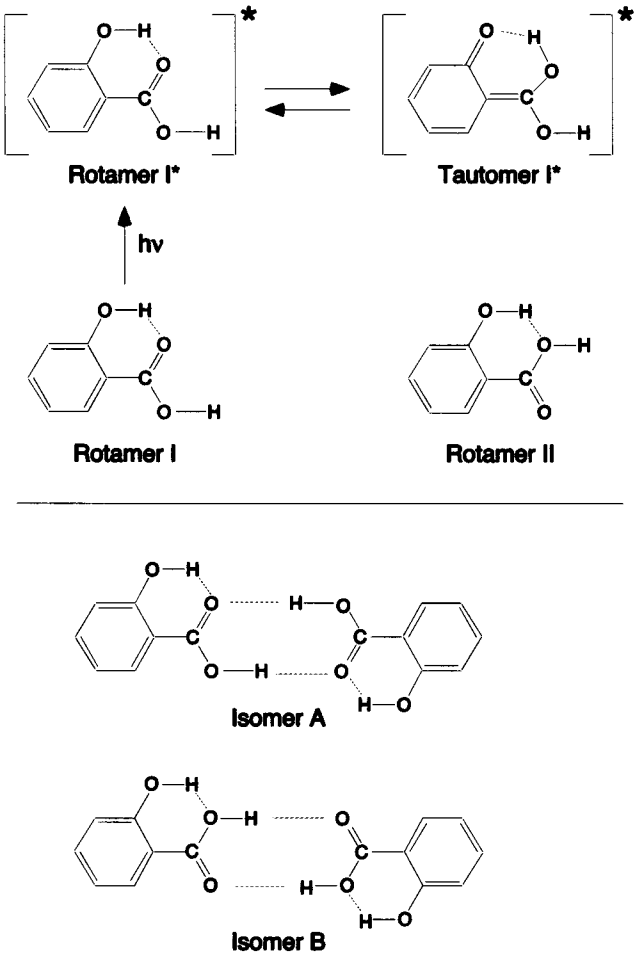

Figure 1. Schematic representation for the structure of salicylic acid (SA) in (upper) monomer and (lower) dimer.

10.1021/jp0126199 CCC: $20.00
Published on Web 11/03/2001

and dispersed fluorescence spectra of the SA dimer and of the clusters with several solvent molecules.[13,14] They concluded that isomer A was the sole structure in the S_0 state, on the basis of the spectral shift of the origin band of the S_1-S_0 transition.

The structure of SA in the S_1 state has also been the subject of various studies.[6−18] Since Weller's pioneering work,[15,16] it has been well-known that SA and its derivatives show ultraviolet and visible fluorescence from the S_1 state.[6−9,17] Such a dual emission is observed not only in solutions but also under an isolated jet-cooled condition.[10−14] The origin of the largely Stokes shifted fluorescence (visible emission) has been attributed to ESIPT from the phenolic OH to the carbonyl group. This ESIPT process is prohibited in rotamer II, and can occur only in rotamer I, as depicted in Figure 1. This transformation is equivalent to an enol−keto tautomerization in the electronic excited state, and here we call the transformation product tautomer I*. Though the original work by Weller proposed a double minimum potential corresponding to rotamer I* (enol) and tautomer I* (keto),[15,16] electronic spectroscopy of jet-cooled SA suggested a single minimum at the tautomer I* form, based on the excitation energy dependence of the ratio of the ultraviolet/visible emission intensities.[10,13,14] Recent high-level ab initio calculations of the S_1 structure of SA also predicted a single minimum in the S_1 (π, π^*) surface.[18] The calculated excited-state minimum corresponded to a shift of the H atom by only about 0.15 Å along the OH bond with respect to the equilibrium position in the S_0 state, and the large Stokes shift of the fluorescence was mainly attributed to the rearrangement of the H-chelate ring. This mechanism is called "proton dislocation" model, which was first proposed by Nagaoka and Nagashima for the case of salicylaldehyde.[17] However, there have been no experimental data to estimate the location of the minimum in the S_1 surface, and the direct evidence about the OH bond is desired for the examination of the model.

In the case of the SA dimer, ESIPT between the phenolic OH and carbonyl groups is prohibited by intermolecular hydrogen bond formation even in isomer A, which is formed by dimerization of rotamer I. However, the fluorescence spectra from the S_1 origin is broadened and extends to the visible region.[10,13,14] This fact suggests two possible cases for the structure of the SA dimer in the S_1 state; one is to accomplish fast equilibrium between isomers A and B (intermolecular double proton transfer), and the other is to exhibit an intermediate structure between A and B. Lahmani and Zehnacker-Rentien observed the absence of the shape evolution of the emission as a function of the excitation energy, and proposed a single minimum S_1 surface-modified relative to that of isomer A.[13]

All of the experimental information about structures of SA and its dimer under a supersonic jet condition has been obtained so far by electronic spectroscopy, which offers only indirect evidence for the structure determination.[10,13,14] The key to the structure determination is clearly to observe the intramolecular and intermolecular hydrogen-bonded OH groups, and infrared (IR) spectroscopy should be the most suitable technique. Recent development of two-color double resonance techniques enables us to apply IR spectroscopy both in the S_0 and S_1 states under jet expansion conditions, and it has been demonstrated that such IR spectroscopy is very powerful for structure determination of hydrogen-bonded clusters.[19−21] In this paper, we report IR spectroscopy of the jet-cooled SA monomer and dimer in the OH stretching vibrational region. Rotamers I and II of the SA monomer are unequivocally assigned on the basis of the observation of the OH stretching vibrations. The SA dimer structure is also determined by the similarity of the IR spectra with those of the monomers. IR spectra in the S_1 state are observed, and the structures in the S_1 state are discussed.

II. Experimental Section

In this study, we utilized infrared−ultraviolet (IR-UV) and ultraviolet−infrared (UV-IR) double resonance spectroscopic techniques to observe the OH vibrations of jet-cooled species in the S_0 and S_1 states, respectively. Both techniques were described in detail elsewhere,[20,22] and only a brief description is given here.

(a) IR-UV Double Resonance Spectroscopy for the S_0 State. A pulsed UV laser whose wavelength is fixed at the origin (0−0) band of the S_1-S_0 transition of the molecule (cluster) is introduced, and the fluorescence signal from the S_1 state is observed as a measure of the S_0 state population. A pulsed IR beam is introduced 50 ns *prior* to the UV laser pulse, and its wavelength is scanned. When the IR wavelength is resonant on a vibrational transition of the molecule (cluster) in the S_0 state, the IR absorption induces a reduction of the population in the ground state, and is detected as a decrease of the fluorescence signal intensity. Thus, by scanning the IR laser wavelength, fluorescence dip spectra which correspond to IR absorption spectra of the S_0 state are obtained.

(b) UV-IR Double Resonance Spectroscopy for the S_1 State. A pulsed UV laser of which wavelength is fixed at the origin band of the S_1-S_0 transition of the molecule (cluster) is introduced, and the fluorescence signal from the vibrational ground level of the S_1 state is monitored. A pulsed IR beam is introduced just *after* the UV laser pulse, and its wavelength is scanned. Whenever the quantum yield of the vibrationally excited level is lower than that of the vibrationally ground level because of the enhancement of nonradiative processes, a decrease of the fluorescence signal intensity occurs as the IR wavelength is resonant on a vibrational transition of the S_1 state. Thus, by scanning the IR laser wavelength, fluorescence dip spectra which correspond to IR absorption spectra of the S_1 state are obtained.

In both the IR-UV and UV-IR spectroscopic technique, the species selection with respect to rotamers and/or cluster sizes is performed by tuning the UV laser wavelength for the electronic transition.

The tunable IR beam was obtained by a difference frequency generation with a $LiNbO_3$ crystal, in which a second harmonic of a Nd:YAG laser (Quanta-Ray GCR230) and an output of a Nd:YAG laser pumped dye laser (Continuum ND 6000) were mixed. The UV light source was a second harmonic of a YAG laser (Spectra Physics Indi) pumped dye laser (Lumonics HD 500). Temporal pulse widths of both lasers were about 8 ns. Accuracy of the laser frequencies was about 0.5 cm^{-1}. The delay time between the two laser pulses was controlled by a digital delay generator (Stanford Research DG 535). The IR beam, focused at 10 mm downstream of a pulsed jet nozzle by a lens ($f = 250$ mm), was counter-propagated to the UV laser beam which was focused by a lens of $f = 500$ mm. Laser-induced fluorescence was passed through glass filters (Corning 7-59 and Toshiba L39), and was detected by a photomultiplier (Hamamatsu R928).

The SA sample was purchased from Tokyo Kasei Co., and was used without further purification. The sample was heated to 360 K, and its vapor was seeded in helium (stagnation pressure of 3 atm). The gaseous mixture was expanded into a vacuum chamber through a pulsed nozzle with an orifice of 0.8 mm diameter.

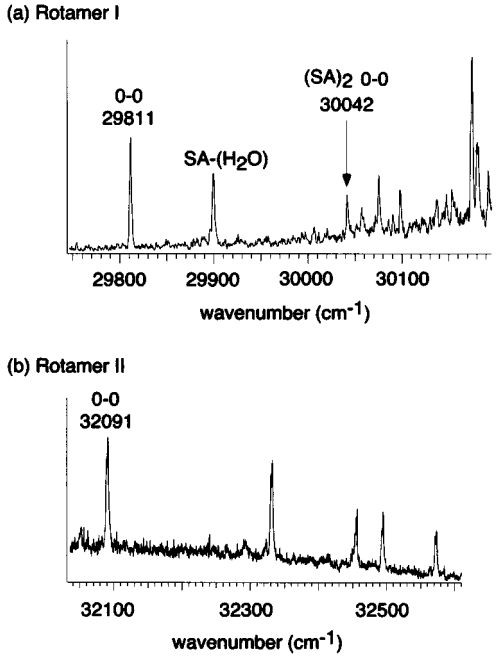

Figure 2. Fluorescence excitation spectra of the S_1-S_0 transitions of jet-cooled SA. (a) Origin band region of rotamer I of the monomer and the dimer. The band at 29900 cm^{-1} is the origin of the SA−water cluster. (b) Origin band region of rotamer II of the monomer. The assignments of the rotamers and clusters were confirmed by IR spectroscopy (see text).

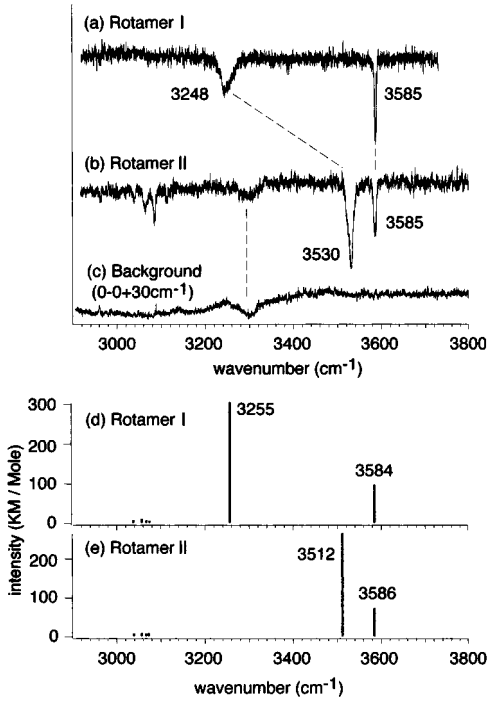

Figure 3. OH stretching vibrational region of the infrared (IR) spectra of (a) rotamer I and (b) rotamer II of jet-cooled SA in the electronic ground (S_0) state. The IR−UV double resonance technique was used to measure the spectra. The origin bands at 29811 cm^{-1} and 32091 cm^{-1} in the electronic transitions were used to probe the ground-state population, respectively. (c) IR spectrum obtained by monitoring the broad background component around the origin band of rotamer II. The UV laser excited (32091+30) cm^{-1}. (d), (e) Simulation of the IR spectra of rotamer I and II, respectively, in the S_0 state. The simulation is based on the optimized structures at the B3LYP/6-31G (d, p) level calculations, and the scaling factor of 0.9522 is applied to the calculated frequencies.

III. Results and Discussion

(a) S_1-S_0 Fluorescence Excitation Spectra of the SA Monomer and Dimer. Figure 2a shows the fluorescence excitation spectrum of jet-cooled SA in the 335 nm region. This spectrum was recorded by monitoring the fluorescence in the range of 400−500 nm. The spectrum of this region was first reported by Bisht et al., and they assigned the lowest-frequency band at 29811 cm^{-1} (in a vacuum-corrected wavenumber) to the origin band (0−0 band) of the S_1-S_0 (π, π^*) transition of rotamer I.[10] This assignment was made on the basis of an analogy to the spectrum of MS,[11,12] in which a similar spectrum is expected. The single vibronic level fluorescence spectrum of this band shows a dual emission, and it has been attributed to ESIPT, which is allowed in rotamer I, but is prohibited in rotamer II. The intensity of the origin band is considerably weak. The Franck−Condon distribution is mainly seen in the region of the vibrational energy over 600 cm^{-1}, and the strongest band appears at +849 cm^{-1} from the origin.[10] These spectral features suggest a substantial geometrical change upon electronic excitation.

Another band system of SA is seen in the 310 nm region, as shown in Figure 2b. Several sharp bands appear with a broad background component. The same spectrum has already been reported by Bisht et al., and the band at 32091 cm^{-1} was assigned to the origin band of the S_1-S_0 (n, π^*) transition of rotamer II.[10] This assignment is also based on the similarity of the spectrum with that of MS.[11,12] In the case of rotamer II, nonbonding electrons (n) of the carbonyl O atom are considered to be free from the intramolecular hydrogen bond with the phenolic OH, thus the electronic configuration of the S_1 state is different from that of rotamer I. The origin band of rotamer II is 2280 cm^{-1} higher in transition energy than that of rotamer I (29811 cm^{-1}). The broad background was attributed to the high-frequency tail of bands due to SA clusters.

The S_1-S_0 origin band of the SA dimer appears at 30042 cm^{-1}, as seen in Figure 2a. Bisht et al. observed that the intensity of this band showed a strong pressure dependence of the SA vapor, and used this fact as evidence for their assignment.[10] The band position of the dimer is much closer to that of the origin of rotamer I (+231 cm^{-1}) than that of rotamer II (−2049 cm^{-1}). This suggests the isomer A structure for the SA dimer because isomer A consists of two molecules in the rotamer I form.[10,13]

(b) OH Stretching Vibrations of the SA Monomers in S_0. Figure 3(a) and (b) show the IR spectra of the SA monomer in the OH stretching vibrational region. Spectra (a) and (b) were measured by monitoring the fluorescence intensities obtained by the 29811 and 32091 cm^{-1} band excitation, respectively, while scanning the IR wavelength. In spectrum (a), a sharp band appears at 3585 cm^{-1}, and a broad one is seen at 3248 cm^{-1}. The sharp band is clearly assigned to the free OH stretch of the carboxylic group. The broad one is attributed to the phenolic OH which is intramolecularly hydrogen-bonded to the neighboring carbonyl group.[22] The phenolic OH frequency has been reported to be 3230 cm^{-1} in the high-resolution dispersed fluorescence study by Bisht et al.[10] The OH frequency of the present IR study provides a more accurate value of the frequency. Since the free OH stretching vibrational frequency of phenol is known to be 3657 cm^{-1},[23] the low-frequency shift of the phenolic OH group due to the intramolecular hydrogen bond is roughly estimated to be 400 cm^{-1}.

In spectrum (b), on the other hand, the intramolecularly hydrogen-bonded phenolic OH band is found at 3530 cm^{-1},

while the free carboxylic OH band shows no shift from 3585 cm^{-1}. The low-frequency shift of the phenolic OH stretch is only about 100 cm^{-1}, and the bandwidth is much sharper than that of the band at 3248 cm^{-1} in spectrum (a). These spectral features indicate that the intramolecular hydrogen bond of the spectral carrier for the electronic transition at 32091 cm^{-1} is much weaker than that for the band at 29811 cm^{-1}.

In IR spectrum (b), three weak bands around 3080 cm^{-1} and a weak and broad dip at 3300 cm^{-1} are seen. The former bands are due to the aromatic CH stretches. To identify the broad band around 3300 cm^{-1}, we have observed the IR spectrum (c) in Figure 3 by monitoring the background fluorescence around the origin band of the 310 nm system (the 32091+30 cm^{-1} region was excited by the UV laser). The background fluorescence is due to higher clusters of SA. Spectrum (c) also shows a weak band at 3300 cm^{-1}, representing that the broad band in spectrum (b) is attributed to the background.

The IR spectra of the OH stretching vibrational region clearly demonstrate a qualitative determination of the rotamers by considering the difference between the intramolecular hydrogen bonds in the two rotamers. It is easily expected that the intramolecular hydrogen bond in rotamer I is stronger than that in rotamer II because the carbonyl O atom is more basic than the carboxylic O atom. Therefore, the spectral carriers of the 29811 and 32091 cm^{-1} bands of the S_1-S_0 transitions are uniquely assigned to rotamers I and II, respectively. This conclusion is consistent with the previous assignments given by Bisht et al., which were based on the similarity of the electronic spectrum with that of MS and their emission properties.[10]

The above qualitative discussion can be confirmed by quantum chemical calculations. We carried out density functional theoretical (DFT) calculations of stable structures of SA in the S_0 state, and simulated their vibrational spectra. The calculations were performed at the B3LYP/6-31G(d, p) level,[24] and the Gaussian 98 program package was used.[25] By assuming C_s symmetry for the molecule, two stable structures corresponding to rotamers I and II were obtained. Their energy optimized structures are shown in Figure 4,[26] and their key structural parameters are tabulated in Table 1. The atom numbers used in Table 1 are defined in Figure 4. The simulated IR spectra based on these structures and harmonic vibrational frequency approximation are shown in Figure 3 (d) and (e). The scaling factor of 0.9522 was applied to the calculated frequencies to fit on the observed band positions. The B3LYP/6-31G(d, p) level calculations well reproduce the observed IR spectra, and the assignments of the rotamers are unequivocally confirmed.

The DFT calculations predicted that rotamer I is more stable (3.914 kcal/mol) than rotamer II in total energy including the zero point energy (ZPE) corrections. The most of the energy difference should be due to the difference in the intramolecular hydrogen bond strength. The calculated phenolic OH stretch frequency in rotamer I is 257 cm^{-1} lower than that of rotamer II (−282 cm^{-1} in the observed spectra), while the carboxylic OH shows almost the same frequency between the rotamers. The calculated phenolic O−H distance (R_{O1-H1} in Table 1) is 0.0141 Å longer in rotamer I than in rotamer II, reflecting the difference of the intramolecular hydrogen bond strength. Other structural parameters in the H-chelate ring also represent difference between the rotamers. The C−O (R_{O2-C3}) and C═O (R_{O3-C3}) distances of the carboxylic group are substantially sensitive to the difference of the conformation. These results indicate that the whole H-chelate ring is strongly affected by the intramolecular hydrogen bond formation.

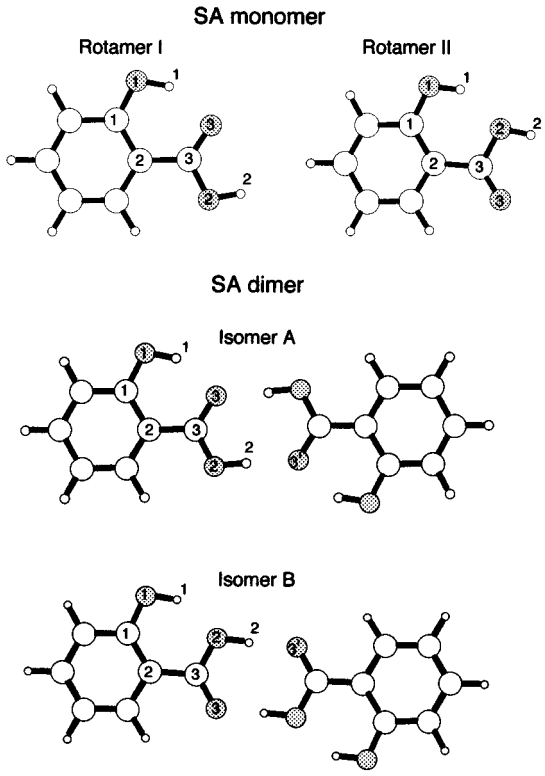

Figure 4. Energy optimized structures of (upper) monomer and (lower) dimer of SA at the B3LYP/6-31G (d, p) level calculations. Numbers in the figure are definitions of atom numbers in Tables 1 and 2. C_s and C_{2h} symmetry is assumed for the monomer and dimer, respectively, in the calculations.

TABLE 1: Key Structural Parameters of the Energy Optimized Structures of the SA Monomer in the S_0 State[a]

Rotamer lI		Rotamer II	
Relative Energy (kcal/mol)			
0		+3.914	
Bond Distance (Å)			
R_{O1-H1}	0.9869	R_{O1-H1}	0.9728
R_{O2-H2}	0.9717	R_{O2-H2}	0.9714
R_{O3-H1}	1.7285	R_{O2-H1}	1.7920
R_{O1-O3}	2.6115	R_{O1-O2}	2.6279
R_{O1-C1}	1.3416	R_{O1-C1}	1.3502
R_{O2-C3}	1.3482	R_{O2-C3}	1.3777
R_{O3-C3}	1.2333	R_{O3-C3}	1.2125
R_{C1-C2}	1.4200	R_{C1-C2}	1.4177
R_{C2-C3}	1.4640	R_{C2-C3}	1.4755
Bond Angle (deg)			
$\Theta_{H1-O1-C1}$	107.16	$\Theta_{H1-O1-C1}$	109.11
$\Theta_{O1-C1-C2}$	122.82	$\Theta_{O1-C1-C2}$	124.72
$\Theta_{C1-C2-C3}$	118.58	$\Theta_{C1-C2-C3}$	124.63
$\Theta_{C2-C3-O3}$	124.49	$\Theta_{C2-C3-O3}$	113.52
$\Theta_{C3-O2-H2}$	106.01	$\Theta_{C3-O2-H2}$	106.36

[a] The calculations were performed at the B3LYP/6-31G(d, p) level. Definitions of atomic numbers are seen in Figure 4.

(c) OH Stretching Vibrations of the SA Dimer in S_0. The IR spectrum of the SA dimer in the S_0 state was obtained when the UV laser wavelength is fixed at 30042 cm^{-1}, which is the origin band of the dimer.[10] Figure 5(a) shows its OH stretching vibrational region. A rather broad band appears at 3295 cm^{-1}, and an extraordinary broad band occurs around 2900 cm^{-1}, accompanied by several sharp bands. No absorption is seen for the free OH stretch region (around 3600 cm^{-1}).

By comparing with the IR spectra of rotamers I and II of the monomer, the band at 3295 cm^{-1} of the dimer is clearly assigned

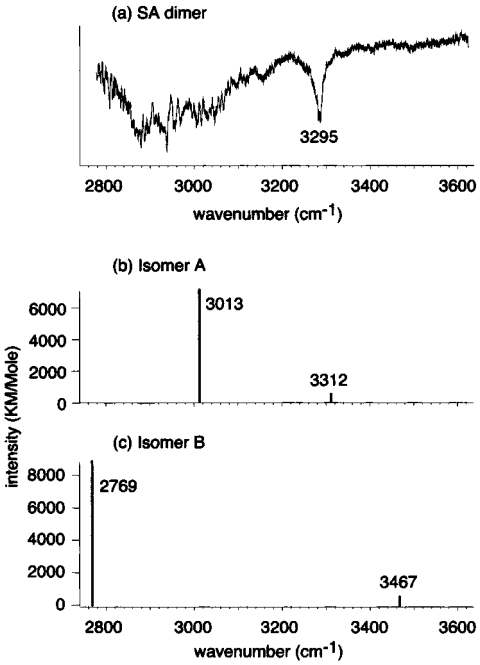

Figure 5. (a) OH stretching vibrational region of the IR spectrum of the SA dimer in the S_0 state. The IR-UV double resonance technique was used to measure the spectrum. The origin band at 30042 cm^{-1} in the electronic transitions was used to probe the ground-state population. (b), (c) Simulation of the IR spectra of the dimer in the isomer A and B structures, respectively. The simulation is based on the optimized structures at the B3LYP/6-31G (d, p) level calculations, and the scaling factor of 0.9522 is applied to the calculated frequencies.

to the phenolic OH which is intramolecularly hydrogen-bonded to the carbonyl group. Therefore, the isomer A structure of the dimer, which essentially consists of a combination of two monomer units of rotamer I, is concluded for the SA dimer in the S_0 state. In this respect, it is noticed that the phenolic OH frequency is high-frequency shifted by 47 cm^{-1} upon the dimer formation. When a strong *intermolecular* hydrogen bond is formed upon the dimerization, the nonbonding electrons of the carbonyl group are strongly attracted by the carboxylic OH group of the other unit, and it reduces the electron density between the phenolic OH and carbonyl O atom, resulting in the decrease of the *intramolecular* hydrogen bond strength.

The broad absorption around 2900 cm^{-1} is assigned to the OH stretching vibration in the $(COOH)_2$ ring bound by the intermolecular hydrogen bonds. Because of the g-u symmetry expected for such a symmetric dimer, only the antisymmetric combination of the carboxylic OH stretching vibrations should be IR active. Though the single OH band should carry the IR absorption intensity in this region, the width of the band is extremely wide ($\sim$200 cm^{-1}). Many sharp bands lying on the broad absorption are attributed to overtone and combination bands mixed with the OH vibrations. A similar feature of the broadening of OH stretching bands has often been seen for strongly hydrogen-bonded dimers, such as pyridone dimer[26,27] and benzoic acid dimer.[28,29]

We also performed DFT calculations of the SA dimer at the same level (B3LYP/6-31G(d, p)) as those for the monomer. By assuming C_{2h} symmetry, energy optimized structures corresponding to isomers A and B were found. The calculated structures are shown in Figure 4, and their key structural parameters are tabulated in Table 2. The simulated IR spectra based on the optimized structures are presented in Figure 5 (b) and (c). The same scaling factor (0.9522) as that for the monomer was applied to the calculated vibrational frequencies.

TABLE 2: Key Structural Parameters of the Energy Optimized Structures of the SA Dimer in the S_0 State[a]

Isomer A		Isomer B	
Relative Energy (kcal/mol)			
0		+3.921	
Bond Distance (Å)			
R_{O1-H1}	0.9837	R_{O1-H1}	0.9754
R_{O3-H1}	1.7356	R_{O2-H1}	1.7775
R_{O1-O3}	2.6109	R_{O1-O2}	2.6203
R_{O2-H2}	1.0036	R_{O2-H2}	1.0190
$R_{O3'-H2}$	1.6413	$R_{O3'-H2}$	1.5573
$R_{O2-O3'}$	2.6446	$R_{O2-O3'}$	2.5760
R_{O1-C1}	1.3426	R_{O1-C1}	1.3469
R_{O2-C3}	1.3161	R_{O2-C3}	1.3339
R_{O3-C3}	1.2547	R_{O3-C3}	1.2381
R_{C1-C2}	1.4202	R_{C1-C2}	1.4193
R_{C2-C3}	1.4646	R_{C2-C3}	1.4713
Bond Angle (deg)			
$\Theta_{H1-O1-C1}$	107.20	$\Theta_{H1-O1-C1}$	108.59
$\Theta_{O1-C1-C2}$	123.15	$\Theta_{O1-C1-C2}$	124.40
$\Theta_{C1-C2-C3}$	119.91	$\Theta_{O1-C1-C2}$	123.43
$\Theta_{C2-C3-O3}$	121.88	$\Theta_{C2-C3-O2}$	115.33
$\Theta_{C3-O2-H2}$	110.61	$\Theta_{C3-O2-H2}$	111.56

[a] The calculations were performed at the B3LYP/6-31G(d, p). Definitions of atomic numbers are seen in Figure 4.

In comparison with the observed and simulated IR spectra of the SA dimer, it is evident that the observed IR spectrum is reproduced very well with the isomer A structure than the isomer B structure, supporting the conclusion from the qualitative discussion described above. The band at 3312 cm^{-1} in the simulation of isomer A is the antisymmetric combination of the phenolic OH stretches, and the band at 3013 cm^{-1} is that of the $(COOH)_2$ ring. The calculated frequency splitting between the symmetric (IR-inactive) and antisymmetric (IR-active) combinations is 1.6 cm^{-1} in the phenolic OH stretches and 97.0 cm^{-1} in the $(COOH)_2$ ring. The splitting indicates that the phenolic OH stretch is essentially isolated in each unit while the carboxylic OH stretches strongly interact with each other.

The simulated IR spectrum of isomer A well reproduces the observed high-frequency shift of the phenolic OH stretch upon the cluster formation. As was discussed above, the intermolecular hydrogen bond formation would cause a decrease of the intramolecular hydrogen bond strength, resulting in the high-frequency shift. The DFT calculations demonstrate that the phenolic O−H bond distance (R_{O1-H1}) is shortened for 0.0032 Å upon the cluster formation. The very small frequency splitting between the symmetric and antisymmetric phenolic OH stretches denies an alternative explanation that the high-frequency shift is caused by the interaction between the two phenolic OH stretches.

In the case of the isomer B structure, the OH stretch band of the $(COOH)_2$ ring is extremely lower-frequency shifted than that of isomer A, corresponding to much stronger intermolecular hydrogen bond formation. At the B3LYP/6-31G(d, p) level calculations, the stabilization energy due to the dimer formation (intermolecular hydrogen bonds) is estimated to be 19.776 kcal/mol for isomer B, while that for isomer A is 14.308 kcal/mol (including the ZPE and basis set superposition error corrections). The calculated carboxylic O−H bond distance (R_{O2-H2}) is also 0.0083 Å longer in isomer B than that in isomer A, as seen in Table 2. On the other hand, the total energy including the ZPE corrections is evaluated to be lower (3.921 kcal/mol) in isomer A than isomer B. Isomer A essentially consists of two monomer units of rotamer I, which is estimated to be 3.914 kcal/mol more stable than rotamer II because of the stronger intramolecular

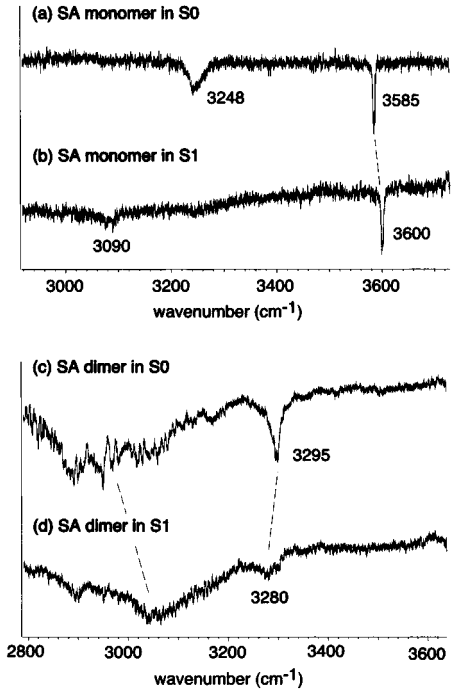

Figure 6. (upper) Comparison of the IR spectra of rotamer I of SA in the (a) S_0 and (b) S_1 states. Spectrum (a) is the reproduction of spectrum (a) of Figure 3. Spectrum (b) was obtained by using the UV-IR technique. The UV laser excited the molecule to the vibrational ground level of the S_1 state. (lower) Comparison of the IR spectra of the SA dimer in the (c) S_0 and (d) S_1 states. Spectrum (c) is the reproduction of spectrum (a) of Figure 5. Spectrum (d) was obtained by the UV-IR technique. The UV laser excited the molecule to the vibrational ground level of the S_1 state.

hydrogen bond. Although the intermolecular hydrogen bond stabilization energy of isomer A is estimated to be much less than that of isomer B, the larger stabilization energy originating from the intramolecular hydrogen bond of the rotamer I units leads to the larger total stabilization energy for isomer A.

(d) OH Stretching Vibrations of the SA Monomer in S_1. The IR spectrum of the SA monomer in S_1 is shown in Figure 6 (b). The IR spectrum in S_0 is also reproduced in Figure 6 (a) for a comparison. In IR spectrum (b), the UV laser excitation of the origin band (29811 cm^{-1}) prepares the ground vibration level of S_1 of the SA monomer (rotamer I), then the IR laser wavelength was scanned by monitoring the fluorescence intensity. For the S_1 state of rotamer I, Bisht et al. reported that a nonradiative decay process takes place with an activation energy of 1100 cm^{-1} above the zero-point level.[10] Therefore, the fluorescence depletion occurs when the IR laser excites the molecule in S_1 to vibrationally excited levels higher than 1100 cm^{-1}. The IR spectrum in S_1 shows a sharp absorption at 3600 cm^{-1}, and a weak band at 3090 cm^{-1}. The baseline depletion below 3500 cm^{-1} is an artifact due to the fluctuation of the jet nozzle condition, and no broad absorption was observed below 3500 cm^{-1} under the present detection sensitivity.

The sharp band at the 3600 cm^{-1} in S_1 is clearly assigned to the free carboxylic OH stretching vibration. The frequency shows a high-frequency shift of 15 cm^{-1} upon the electronic excitation. Though the reduction of the carboxylic OH acidity upon the electronic excitation has been pointed out,[13,30] the free OH stretching band does not show a significant difference in its vibrational frequency. The weak band at the 3090 cm^{-1} is attributed to the CH stretch of the aromatic ring. A slight high-frequency shift of the aromatic CH stretches has been observed in the electronic excitation of benzene and toluene.[31,32]

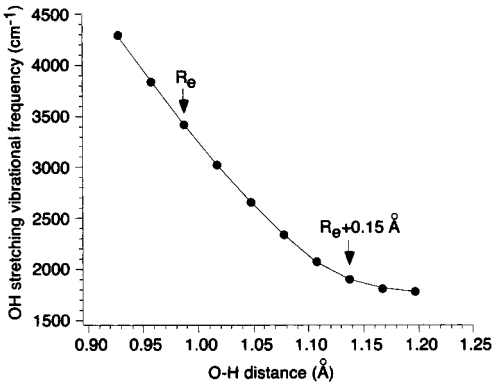

Figure 7. Calculated O−H distance dependence of the phenolic OH stretching vibrational frequency of rotamer I of SA in the S_0 state (see text). The calculations were performed at the B3LYP/6-31G(d, p) level. No scaling factor was applied to the calculated vibrational frequency. R_e indicates the equilibrium O−H distance in this level of the calculations.

A remarkable difference between the IR spectra in the S_0 and S_1 states is seen with respect to the phenolic OH stretch; the intramolecularly hydrogen-bonded OH occurs at 3248 cm^{-1} in S_0, but it disappears in the S_1 spectrum. Though we carefully examined the lower-frequency region down to the limit of the difference frequency mixing (2400 cm^{-1}), no sign of the phenolic OH in the S_1 state was found. This fact clearly indicates that a drastic change of the intramolecular hydrogen bond occurs upon the electronic excitation.

For the fluorescence from the S_1 state of SA, a large Stokes shift has been known, both in the gas and condensed phases,[6−17] and it has been attributed to ESIPT between the phenolic OH and the carbonyl group. On the other hand, however, recent high level ab initio calculations of the S_1 state by Sobolewski and Domcke predicted that the S_1 minimum corresponds to an elongation of the phenolic OH bond by only 0.15 Å with respect to the equilibrium in S_0, and most of the Stokes shift of the fluorescence arises from the rearrangement of the H-chelate ring.[18] Though such a displacement of the H atom does not mean its transfer to the carbonyl site, as is seen from Figure 4 and Table 1, it may lead to significant reduction of the OH stretching vibrational frequency. To estimate the frequency reduction, we calculated the O−H distance dependence of the OH stretching vibrational frequency in S_0. We obtained the energy-optimized structure of rotamer I at the B3LYP/6-31G(d, p) level, and calculated the OH stretching vibrational frequencies by changing only the O−H distance of the phenolic OH, which are summarized in Figure 7. No scaling factor is applied to the calculated frequencies. The OH frequency remarkably decreases with increase of the O−H distance; the OH frequency is 3419 cm^{-1} at the equilibrium O−H distance (0.9869 Å) in this level of the calculation, and it decreases to 1902 cm^{-1} with an increase of the O−H distance only by 0.15 Å. Though this calculation is made for the electronic *ground* (S_0) state, it is reasonable to expect a similar decrease of the OH frequency even for the S_1 state. Thus, it is evident that the disappearance of the phenolic OH in the region of 2400−3600 cm^{-1} is consistent with the prediction by Sobolewski and Domcke.[18] The similar small H atom displacement model has been first pointed out for salicylaldehyde by Nagaoka and Nagashima.[17] In the case of MS, which is also known to show the large Stokes shift in the S_1 fluorescence, the OH stretch frequency was roughly estimated to be 2600 cm^{-1} based on the deuteration shift of the electronic transition.[12]

When the UV laser excited the vibrational level of +849 cm^{-1}, which is the Franck−Condon maximum in the in the S_1−

S_0 transition of rotamer I,[10] no change of the IR spectrum of the S_1 state was observed in the range of 2900−3600 cm^{-1}; only the free carboxylic OH band is seen in the spectrum and the phenolic OH band disappears. This fact is consistent with the single minimum surface of the S_1 state, which has been suggested by vibrational energy dependence of the fluorescence.[10]

The Stokes shift of the S_1 fluorescence of SA has long been interpreted with the ESIPT process.[6−9,15,16] When ESIPT occurs in rotamer I, it results in the production of tautomer I* which has two carboxylic OH groups, as schematically shown in Figure 1. Though such ESIPT (or enol−keto tautomerization) has been pointed out for many molecules, there has been no direct observation of OH stretching vibrations after the proton transfer (tautomerization) in the gas phase. At present, there is no information on the OH stretching frequency of the intramolecularly hydrogen-bonded carboxylic OH in the tautomer I*, and it is difficult to judge whether the observed IR spectrum of the S_1 state is consistent with the conventional ESIPT interpretation.

In conclusion, the observed IR spectra in S_1 are reasonably interpreted by the phenolic O−H bond stretch of only 0.15 Å predicted by the ab initio calculations,[18] while the possibility of the conventional ESIPT is not eliminated by the IR spectrum. Though there is still a technical problem in the IR light generation, probing of the lower-frequency region in which not only the low-frequency shifted OH stretch but also the CO stretch bands are expected to occur, is required to give a definite conclusion on the structure of the SA monomer in the S_1 state.

(e) OH Stretching Vibrations of the SA Dimer in S_1. The IR spectrum of the SA dimer in S_1 is shown in Figure 6 (d). An extremely broad band appears around 3050 cm^{-1}, and two clear shoulders are seen at 2900 and 3280 cm^{-1}. The spectral feature is similar to that in S_0 reproduced in Figure 6 (c). The bands in the S_1 spectrum can be assigned in comparison with those of S_0; the broad absorption around 3050 cm^{-1} is attributed to the antisymmetric OH stretching vibration of the $(COOH)_2$ ring, and the band at 3280 cm^{-1} is assigned to the intramolecular hydrogen-bonded phenolic OH stretch. The shoulder at 2900 cm^{-1} would be attributed to a combination band which borrows the intensity through the coupling with the OH stretch of the $(COOH)_2$ ring.

As was confirmed by the IR spectrum, the SA dimer in S_0 has the isomer A structure. If the double proton transfer (isomerization from isomer A to B) really occurs in S_1, the intramolecular hydrogen bond of the phenolic OH should be weakened, and it should result in a high-frequency shift of the phenolic OH stretch band, as is expected by the comparison between the observed IR spectra of rotamers I and II in S_0 and also between the calculated IR spectra of isomers A and B of the dimer. However, the observed phenolic OH stretch shows a small low-frequency shift (about 15 cm^{-1}) upon the electronic excitation. Therefore, the IR spectra of the SA dimer dispute the double proton transfer in S_1, and it is concluded that the isomer A structure is essentially held in S_1. This is consistent with the previous fluorescence studies of the jet-cooled dimers; the S_1 fluorescence of the dimer shows a much smaller Stokes shifted component than the monomer (rotamer I), and no excitation energy dependence of the intensity of the Stokes shifted component is found.[10,13]

The appearance of the phenolic OH band in the S_1 spectrum of the dimer is quite different from the disappearance of the band in rotamer I in S_1. In the case of the dimer, the carboxylic OH is strongly bound to the carboxyl O atom of the second SA molecule by the intermolecular hydrogen bond, and it substantially reduces the intramolecular hydrogen bond strength.

The OH stretching vibration of the $(COOH)_2$ ring shows a high-frequency shift of about 100 cm^{-1}. This shift indicates the decrease of the intermolecular hydrogen bond strength, and it is consistent with the high-frequency shift of the band origin upon dimerization. The change of the intermolecular hydrogen bond strength is determined by the balance between the decrease of the acidity of the carboxylic group and the increase of the basicity of the carbonyl group upon the electronic excitation.[13,30]

IV. Summary

Infrared spectroscopy was applied to the monomer and the dimer of salicylic acid under the jet-cooled condition, and their OH stretching vibrations were observed for both the S_0 and S_1 states. Two rotamers of the monomer which have been distinguished in the electronic transitions showed quite characteristic IR spectra of the OH stretching vibrational region, and the firm assignments of the conformations were given in combination with theoretical calculations. The structure of the dimer was also determined on the basis of the observation of the OH stretching vibrations. The phenolic OH stretching band of the monomer disappears upon the electronic excitation, indicating a drastic change of the intramolecular hydrogen bond. The disappearance of the band was reasonably interpreted by the significant low-frequency shift due to the H-atom dislocation, which has been predicted by the theoretical calculations. The IR spectra of the dimer in the S_1 state was similar to that of the S_0 state, and it was concluded that the feature of the dimer structure with respect to both inter- and intramolecular hydrogen bonds remains unchanged upon the electronic excitation. This conclusion denied the possibility of the double proton transfer in S_1.

It has been pointed out that not only displacement of the H atom but also the distortion of the whole H-chelate ring plays an important role in the Stokes shift of the fluorescence from the S_1 state of SA.[17,18] To probe the distortion of the H-chelate ring, observation of the lower-frequency region is very important, though there is still technical difficulty in generation of coherent IR light in this region.

In this paper, we described on the application of IR spectroscopy to the monomer and the homo dimer in a supersonic jet. IR spectroscopy of heterodimers of SA and various solvent molecules has also been carried out in our laboratory. Microsolvation effects on the intramolecular hydrogen bond of SA will be discussed in elsewhere.[33]

Acknowledgment. The authors gratefully acknowledge Dr. H. Ishikawa and Dr. T. Maeyama for helpful discussions.

References and Notes

(1) Kovi, P. J.; Miller, C. L.; Schulman, S. G. *Anal. Chim. Acta* **1972**, *61*, 7.

(2) Bacon, G. E.; Jude, R. J. Z. *Kristallogr.* **1973**, *138*, 19.

(3) Morsi, S. E.; Williams, J. O. *J. Chem. Soc., Perkin Trans.* **1978**, *II*, 1281.

(4) Wojcik, M. *Chem. Phys. Lett.* **1981**, *83*, 503.

(5) Fischer, P.; Jolliker, P.; Meier, B. H.; Ernst, R. R.; Hewat, A. W.; Jorgensen, J. D.; Rotella, F. J. J. *Solid State Commun.* **1986**, *61*, 103.

(6) Joshi, H. C.; Tripathi, H. B.; Pant, T. C.; Pant, D. D. *Chem. Phys. Lett.* **1990**, *173*, 83.

(7) Pant, D. D.; Joshi, H. C.; Bisht, P. B.; Tripathi, H. B. *Chem. Phys.* **1994**, *185*, 137.

(8) Golubev, N. S.; Denisov. G. S. *J. Mol. Struct.* **1992**, *270*, 263.

(9) Denisov, G. S.; Golubev, N. S.; Schreiber, V. M.; Shajakhmedov, S. S.; Shurukhina, A. V. *J. Mol. Struct.* **1996**, *381*, 73.

(10) Bisht, P. B.; Petek, H.; Yoshihara, K.; Nagashima, U. *J. Chem. Phys*. **1995**, *103*, 5290.

(11) Heimbrook, L. N.; Kenny, J. E.; Kohler, B. E.; Scott, G. W. *J. Chem. Phys*. **1981**, *75*, 5201.

(12) Heimbrook, L. N.; Kenny, J. E.; Kohler, B. E.; Scott, G. W. *J. Phys. Chem*. **1983**, *87*, 280.

(13) Lahmani, F.; Zehnacker-Rentien, A. *Chem. Phys. Lett*. **1997**, *271*, 6.

(14) Lahmani, F.; Zehnacker-Rentien, A. *J. Phys. Chem. A* **1997**, *101*, 6141.

(15) Weller, A. *Z. Elektrochem*. **1956**, *60*, 1144.

(16) Weller, A. *Prog. React. Kinet.* **1961**, *1*, 187.

(17) Nagaoka, S.; Nagashima, U. *Chem. Phys*. **1989**, *136*, 153.

(18) Sobolewski, A. L.; Domcke, W. *Chem. Phys*. **1998**, *232*, 257.

(19) Zwier, T. S. *Annu. Rev. Phys. Chem*. **1996**, *47*, 205.

(20) Ebata, T.; Fujii, A.; Mikami, N. *Int. Rev. Phys. Chem*. **1998**, *17*, 331.

(21) Brutschy, B. *Chem. Rev*. **2000**, *100*, 3891.

(22) Mitsuzuka, A.; Fujii, A.; Ebata, T.; Mikami, N. *J. Phys. Chem. A* **1998**, *102*, 9779.

(23) Watanabe, T.; Ebata, T.; Tanabe, S.; Mikami, N. *J. Chem. Phys*. **1996**, *105*, 408.

(24) Stevens, P. J.; Devlin, F. J.; Chablowski, C. F.; Frisch, M. J. *J. Phys. Chem*. **1994**, *98*, 11623.

(25) Frisch, M. J.; Trucks, G. W.; Schlegel, H. B.; Gill, P. M. W.; Johnson, B. G.; Robb, M. A.; Cheeseman, J. R.; Keith, T.; Petersson, G. A.; Montgomery, J. A.; Raghavachari, K.; Al-Laham, M. A.; Zakrzewski, V. G.; Ortiz, J. V.; Foresman, J. B.; Cioslowski, J.; Stefanov, B. B.; Nanayakkara, A.; Challacombe, M.; Peng, C. Y.; Ayala, P. Y.; Chen, W.; Wong, M. W.; Andres, J. L.; Replogle, E. S.; Gomperts, R.; Martin, R. L.; Fox, D. J.; Binkley, J. S.; Defrees, D. J.; Baker, J.; Stewart, J. P.; Head-Gordon, M.; Gonzalez, C.; Pople, J. A. *Gaussian 94*, Rev. D.4; Gaussian, Inc.: Pittsburgh, PA, 1995.

(26) These calculated structures are visualized by using *MOLCAT*, ver.2.5.2: Tsutui, Y.; Wasada, H. *Chem. Lett*. **1995**, 517.

(27) Matsuda, Y.; Ebata, T.; Mikami, N. *J. Chem. Phys*. **1999**, *110*, 8397.

(28) Matsuda, Y.; Ebata, T.; Mikami, N. *J. Chem. Phys*. **2000**, *113*, 573.

(29) Watanabe, T.; Sakai, M.; Saeki, M.; Ishiuchi, S.; Fujii, M. *Abstracts of Conference on Molecular Structures*, Tokyo, 2000.

(30) Zwier, T. S. *Abstracts of the 2000 International Chemical Congress of Pacific Basin Societies*, Honolulu, Hawaii, 2000.

(31) Baum, J. C.; McClure, D. S. *J. Am. Chem. Soc*. **1979**, *101*, 2340.

(32) Page, R. H.; Shen. Y. R.; Lee, Y. T. *J. Chem. Phys*. **1988**, *88*, 5362.

(33) Minejima, C.; Ebata, T.; Mikami, N. To be published.

(34) Yahagi, T.; Fujii, A.; Ebata, T.; Mikami, N. To be published.